# Mechanically Flexible Dielectric Waveguides and Bandstop Filters in Glass Technology at G-band

Thomas Galler, Malte Schulz-Ruhtenberg, Tobias Chaloun, and Christian Waldschmidt



DOI: 10.23919/EuMC54642.2022.9924350

# Mechanically Flexible Dielectric Waveguides and Bandstop Filters in Glass Technology at G-band

Thomas Galler#1, Malte Schulz-Ruhtenberg*2, Tobias Chaloun#3, and Christian Waldschmidt#4
#Institute of Microwave Engineering, Ulm University, 89081 Ulm, Germany
*LPKF Laser & Electronics AG, 30827 Garbsen, Germany
{1thomas.galler, 3tobias.chaloun, 4christian.waldschmidt}@uni-ulm.de, 2malte.schulz-ruhtenberg@lpkf.com

***Abstract*— A novel mechanically flexible filter integrated in a glass dielectric waveguide is presented for sensor applications at G-band (140–220 GHz). The use of laser-induced deep etching (LIDE) technology enables the production of via holes and thus the local modulation of the effective permittivity in a dielectric waveguide. This approach enables the implementation of a filter without the use of metal structures. In addition, extraordinary mechanical flexibility is achieved through meandering slots, which simultaneously perform the permittivity modulation. The RF performance was studied in full-wave simulations and validated by measurements of the manufactured bandstop prototypes. The experimental results of the implemented filter element show good agreement with the simulated values. At the center frequency of 156 GHz a notch depth below –14 dB in the measured stop band is achieved. Additional measurements show a stable filter characteristic at up to $8^\circ$ bend angle applicable for the use as a low-loss waveguide under harsh environmental conditions.**

***Keywords*— Filter, glass, dielectric waveguide, millimeter wave, TGV.**

## I. Introduction

The frequency range above 150 GHz has attracted strong interest for high-resolution radars due to the large available absolute bandwidth and low cost monolithic microwave integrated circuits (MMICs). Therefore, cheap and compact packaging concepts, antennas and waveguide transitions for industrial applications like level measurements in tanks are needed [2]. However, this places high demands on the assembly and integration technology [3], especially for applications in harsh environmental scenarios with high temperature, humidity or pressure. Organic materials like PEEK ($\varepsilon_r' = 3.2$), or HDPE ($\varepsilon_r' = 2.78$) as presented in [4], are not suitable for such conditions, as they show disadvantages in mechanical stability and water resistance. Under the influence of temperature, HDPE leads to strong mechanical deformation.

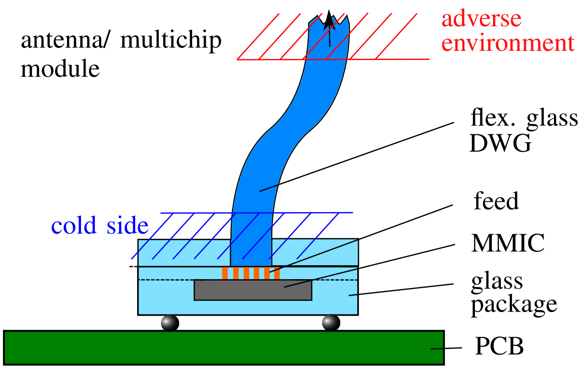


Fig. 1. Radar sensor in glass package [1], feeding a flexible-glass DWG at 160 GHz. This establishes a connection to an antenna or a multichip module.

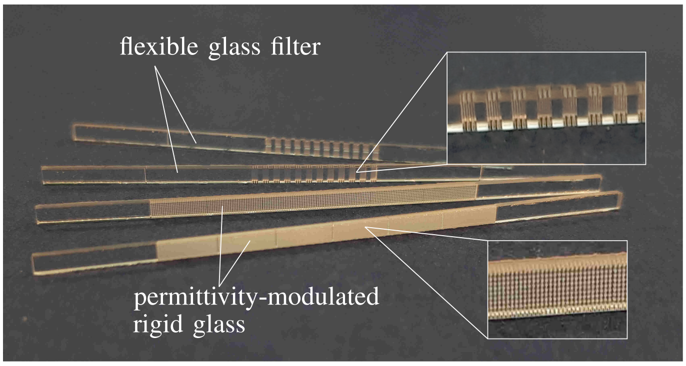


Fig. 2. Flexible-glass bandstop filters and rigid glass, using via holes to locally modulate the effective permittivity.

This paper presents for the first time a flexible-glass dielectric waveguide (DWG) for the G-band, with the option of a direct integration of filters. The filter is manufactured by the laser-induced deep etching (LIDE) process [5], which enables an efficient and low-cost assembly. Unlike recently published designs [6], [7], [8], the presented design enables a local modulation of the waveguide impedance without the use of metallic structures, since the local effective permittivity of the dielectric waveguide substrate material is modified. As the DWG is intended to be used in heat-sensitive environments to bridge thermal distances between the radiating antenna and the hermetically sealed radar sensor package (see Fig. 1), a thermally robust design is achieved as glass has a low thermal expansion coefficient.

In addition, the use of meandering slot structures enables the production of mechanically flexible filter structures, as seen in Fig. 2. Due to this property, small adjustments can be made resulting in a minimal effort for an exact positioning accuracy in the radar sensor module.

## II. Permittivity Modulation in Glass

Due to its electrical and mechanical properties, glass offers excellent opportunities for applications in the millimeter wave frequency band. The complex dielectric properties are

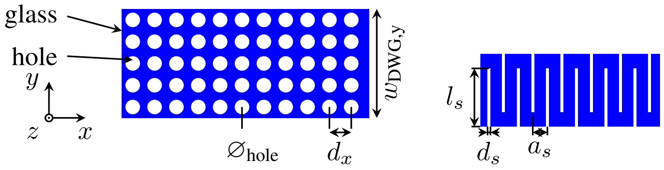


(a) (b)

Fig. 3. Permittivity modulation and flexibility achieved by (a) arrays of circular through-glass holes and (b) meandering slots.

determined by the composition of the glass and its mineral components. Fused silica ($\varepsilon_r' = 3.78$ [9]) has a lower permittivity and a lower dielectric loss factor than borosilicate glass BF33 ($\varepsilon_r' = 4.29$). This property can be locally modified by structuring holes in the glass, as illustrated in Fig. 3(a). Another possibility is to use meandering slots to also achieve mechanical flexibility as shown in Fig. 3(b). As a result, a mixed permittivity $\varepsilon'_{\mathrm{r,mixed}}$ of glass and air ($\varepsilon_r' = 1$) is achieved at the modified region in the DWG. The insertion of holes leads to a local increase of the guided wavelength $\lambda_{\mathrm{G}}$ compared to the unmodified substrate material. To avoid disturbances in the guided wave, the holes have a diameter of less than $\lambda_{\mathrm{G}}/10$. Using the presented fabrication technology, the formation of mechanical cracks is prevented which allows the DWG to be thinned up to a proportion of air of 40%. The measured variation of the local permittivity using BF33 glass is shown in Fig. 4. By inserting holes in the glass, an air content of 10% and 15% was realized, while the mechanical stability is fully maintained.

## III. Glass Filter in a DWG

The demonstrated technique for permittivity modulation is now used to implement a filter by selectively modifying the wave impedance. By means of a suitable arrangement of the locally modified impedance sections, filter properties can be implemented in the waveguide similar to the conventional transmission-line-based filter topologies.

### A. *Filter Design*

Based on the permittivity modulation of the glass DWG, a periodic modulation of the guided wavelength is possible according to

$$\lambda_{\mathrm{G}} = \lambda_0 \cdot \frac{1}{\sqrt{\varepsilon_r}} \,. \quad (1)$$

In contrast to the metallic filters [10], [11] operating at lower frequencies, the field components of DWGs are located in the dielectric medium as well as in the surrounding material. Since a mechanically flexible filter design is desired, the modification is made using meandering slots. The initial conditions for the bandstop filter design are modelled from [12]. By means of full-wave simulation, the dimensions of the slot structures, number and distance of the periodic permittivity regions and waveguide dimensions are then determined numerically. Fig. 5(a) shows the electric field distribution along the DWG with the periodic modulated regions at 160 GHz. The wave propagates in the positive $\vec{k}$ direction. The cross-section of the DWG with its corresponding electric field distribution is illustrated in Fig. 5(b).

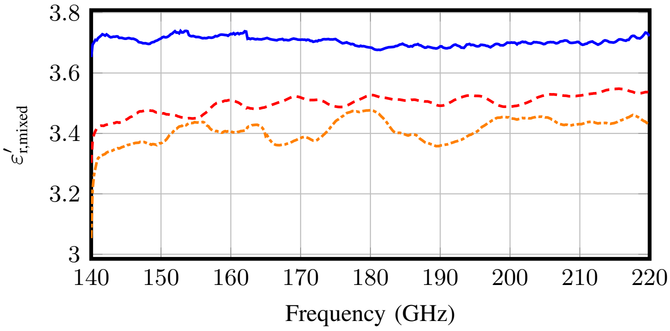


Fig. 4. Measured modulation of the glass permittivity $\varepsilon_r'$ using through glass holes (Unmodulated, 10% air, 15% air).

Table 1. Final dimensions of the glass-based DWG bandstop filter.

| | | | | | |
|---|---|---|---|---|---|
| $\lambda_{\mathrm{G}}$ | 960 µm | $\varnothing_{\mathrm{hole}}$ | 70 µm | $d_{\mathrm{s}}$ | 70 µm |
| $w_{\mathrm{DWG,z}}$ | 648 µm | $d_{\mathrm{x}}$ | 85 µm | $a_{\mathrm{s}}$ | 90 µm |
| $w_{\mathrm{DWG,y}}$ | 1295 µm | $l_{\mathrm{s}}$ | 1150 µm | - | - |

### B. *Fabrication Details*

BF33 glass and fused silica, which are structured using the LIDE process, are investigated to manufacture the filter. The processing is carried out by laser structuring and a subsequent wet etching step. Since the total thickness of the glass wafer decreases homogeneously, the wafer thickness is first deliberately reduced by etching to 730 µm in preparation for the desired final height. Compared to BF33, fused silica offers a four times slower etch rate but a via taper angle of only 0.5° compared to 5° (BF33). Consequently, a higher aspect ratio of the glass via holes can be achieved.

The final dimensions of the glass DWG cross-section then result in 648 µm × 1295 µm, fit for a direct connection to the WR 5.1 standard. Fig. 6(b) shows the finished 4-inch wafer, from which the individual DWGs are then cut out. The mechanical flexibility of the glass with meandering slots is demonstrated in Fig. 6(a). Both, lateral bending in the $y$-direction using the tweezer tips and bending in the $z$-direction, are possible.

Fig. 7 shows the comparison of filters modelled in BF33 and fused silica to the corresponding simulated design. With fused silica, the insertion loss improves by 2.3 dB. At the same time, the stop band notch depth in the frequency range from 150 GHz to 170 GHz differs by 8 dB. Furthermore, the selection of the substrate material is not limited to BF33 or fused silica, as the manufacturing process can readily be applied to other substrate materials such as MEMpax and AF32. The dimensions of the DWG filter are finally listed in Table 1.

## IV. Measurement

The fabricated prototype filter was measured using a network analyser and G-band upconverters. The

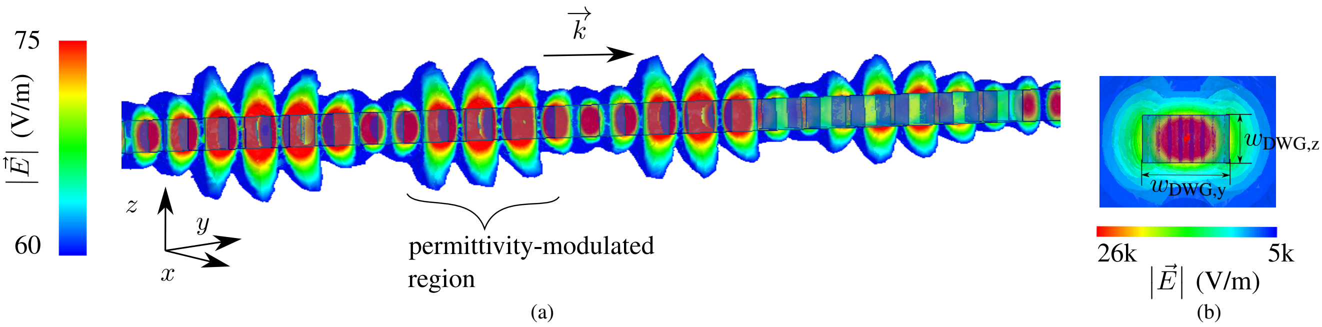


Fig. 5. Electric field distribution of the filter: (a) along the DWG, and (b) in its cross-section.

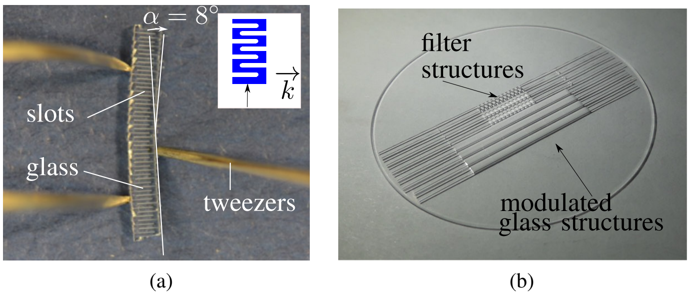


Fig. 6. Structured glass for mechanically flexible DWG: (a) flexible glass DWG bent by $\alpha = 8°$, (b) structured 4-inch wide glass wafer before dicing.

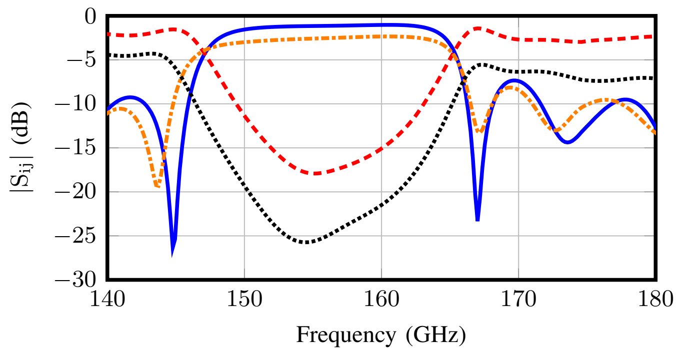


Fig. 7. Simulated scattering parameters of the flexible filter for fused silica and BF33 glass substrate ($|S_{11,\mathrm{FS}}|$, $|S_{21,\mathrm{FS}}|$, $|S_{11,\mathrm{BF33}}|$, $|S_{21,\mathrm{BF33}}|$).

TRL (Through-Reflect-Line) calibration is performed at each waveguide flange. The DWG is then excited via mode converters stimulating the fundamental $\mathrm{HE}_{11}$ mode. Additionally, the influences of the mode converters are removed by means of time-domain gating.

Fig. 8 shows the measurement setup for the characterization of the bandstop filter. A height-adjustable screw is used to determine the influence of a metallic object in the vicinity of the waveguide, as it is later used in tight spaces like radar sensor modules, where proximity to other components is unavoidable. Fig. 9 shows the measurement results for the case without a metallic object. A maximum insertion loss of 14 dB and a return loss of 3.2 dB in the stop band of the filter can be determined. The center frequency is shifted to 155 GHz compared to the simulation, which is caused by the increased slot spacing due to etching tolerances (10%). In Fig. 10, the results with different distances between the metal object and the waveguide are presented. Up to spacings of 1 mm, almost no influence can be detected, since the electromagnetic field components are closely bound to the waveguide. A similar result has already been shown in [4] for a DWG fabricated in HDPE.

Table 2. Comparison to state-of-the-art filter designs.

| Ref. | $f_0$ (GHz) | Filter type | IL (dB) | RL (dB) | Mech. flex. | Diel. material |
|---|---|---|---|---|---|---|
| This work | 156 | bandstop | 14 | 3.2 | yes | glass |
| [10] | 75 | lowpass | 4 | 18 | yes | HIPS |
| [11] | 60 | bandpass | 1.5 | 28 | no | quartz |
| [13] | 4.82 | bandpass | 1.1 | 20 | no | E6045 |

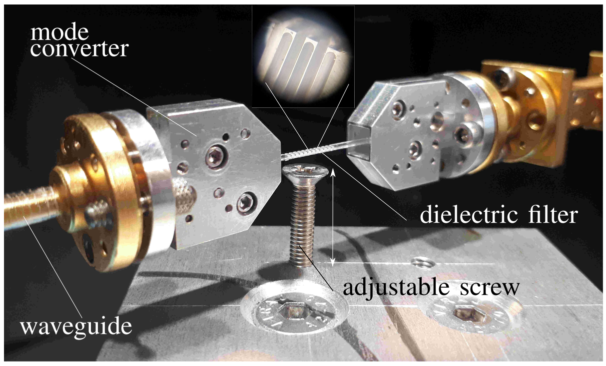


Fig. 8. Measurement setup for the characterization of the glass filter using waveguide standards and mode converters for the stimulation of the fundamental $\mathrm{HE}_{11}$ mode.

The mechanical flexibility of the dielectric glass waveguide is characterized using the measurement setup illustrated in Fig. 11. A secure connection is achieved by a clamp connection of the DWG in the mode converter. A constructed bend is achieved by vertically varying the height $\Delta z$ of the mode converter and thus the end of the glass waveguide. The S-shaped excursion of the waveguide is measured with a dial gauge. A maximum deflection of 3.2 mm over a DWG length of 15 mm is reached before the glass breaks. At the same time, minor variations of the filter characteristics can be observed, as illustrated in Fig. 12. A comparison of these results to other state-of-the-art dielectric filter solutions is given in Table 2.

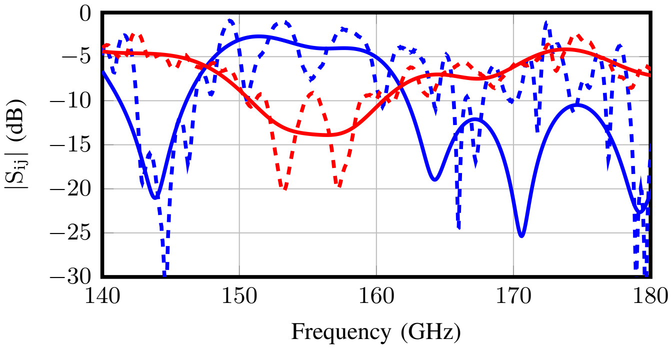


Fig. 9. Measured scattering parameters of the flexible filter realized in fused silica ($|S_{11}|$, $|S_{11,\mathrm{gated}}|$, $|S_{21}|$, $|S_{21,\mathrm{gated}}|$).

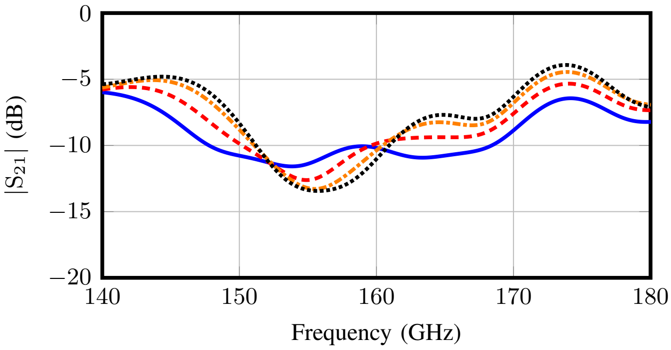


Fig. 10. Measured transmission coefficient for the glass filter at different distances to a metallic object (0.3 mm, 0.5 mm, 1 mm, 2 mm).

## V. Conclusion

In this paper a novel dielectric glass waveguide with integrated bandstop filter without metallic structures above 150 GHz is presented. The combined integration of mechanical flexibility and local permittivity modulation by via holes results in highly robust devices fit for the integration in high temperature sensor applications. This has been verified by the realization and characterization of the bandstop filter entirely without the use of metallic structures. The filter prototype is fabricated in fused silica with WR5.1 waveguide dimensions. A maximum bending angle of $\alpha = 8°$ is achieved. The measured values are in good agreement to the simulation results.

## Acknowledgment

This work was funded by the VDI/VDE Innovation + Technik GmbH within the project GlaRA. – 16ES0692

## References


[1] T. Galler *et al.*, "Glass Package for Radar MMICs Above 150 GHz," *IEEE Journal of Microwaves*, pp. 1–11, 2021.

[2] D. Brumbi, "Low power FMCW radar system for level gaging," in *2000 IEEE MTT-S International Microwave Symposium Digest (Cat. No.00CH37017)*, vol. 3, 2000, pp. 1559–1562 vol.3.

[3] A. Bhutani *et al.*, "122 GHz FMCW Radar System-in-Package in LTCC Technology," in *2019 16th European Radar Conference (EuRAD)*, 2019, pp. 373–376.


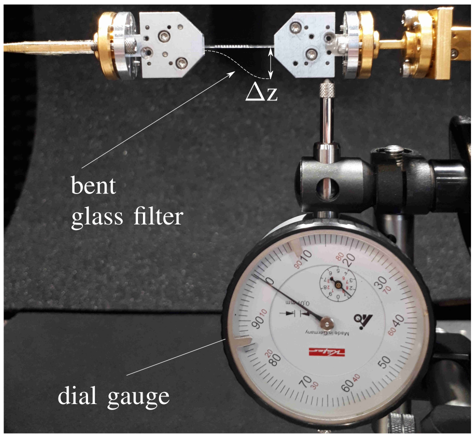


Fig. 11. Measurement setup for the characterization of the mechanical flexibility of the glass DWG.

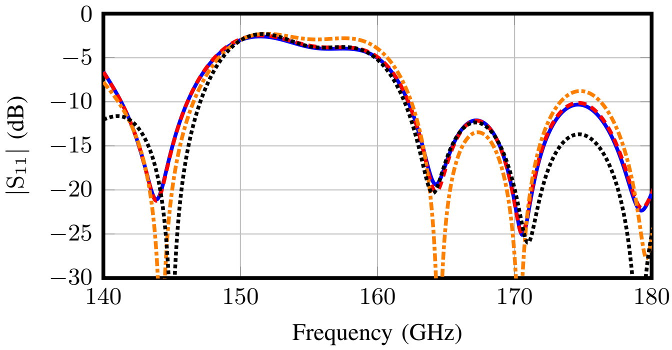


Fig. 12. Measured reflection coefficient of the bent filter at different feed misalignments $\Delta z$ (0.4 mm, 1.2 mm, 2.4 mm, 3.2 mm).


[4] M. Geiger *et al.*, "A 160-GHz Radar With Flexible Antenna Used as a Sniffer Probe," *IEEE Sensors Journal*, vol. 17, pp. 5104–5111, 2017.

[5] R. Ostholt *et al.*, "High-throughput via formation in solid-core glass for IC substrates," *MiNaPAD Conference,2017, Grenoble, France*.

[6] J. C. Myers *et al.*, "Embeded filtering in pcb integrated ultra high speed dielectric waveguides using photonic band gap structures," in *2017 IEEE 26th Conference on Electrical Performance of Electronic Packaging and Systems (EPEPS)*, 2017, pp. 1–3.

[7] L. Murphy *et al.*, "Design of V-band dielectric filled waveguide filters with improved loss and suppression of parasitic waves," in *2014 44th European Microwave Conference*, 2014, pp. 1115–1117.

[8] M. Ito *et al.*, "A 60-GHz-band planar dielectric waveguide filter for flip-chip modules," *IEEE Transactions on Microwave Theory and Techniques*, vol. 49, no. 12, pp. 2431–2436, 2001.

[9] T. Galler *et al.*, "High-Gain Millimeter-Wave Holographic Antenna in Package Using Glass Technology," *IEEE Antennas and Wireless Propagation Letters*, vol. 19, no. 12, pp. 2067–2071, 2020.

[10] C. Baer, "Broadband mmWave Filters using Dielectric Waveguide Bends," in *2021 IEEE International Symposium on Antennas and Propagation and USNC-URSI (APS/URSI)*, 2021, pp. 747–748.

[11] K. Ito and K. Sano, "60-GHz band dielectric waveguide filters made of crystalline quartz," in *IEEE MTT-S International Microwave Symposium Digest, 2005.*, 2005, pp. 2087–2090.

[12] J.-S. Hong and M. Lancaster, *Microstrip Filters for RF/Microwave Applications*, 2011.

[13] A. Widaa and M. Höft, "Miniaturized Dual-Band Dual-Mode TM-Mode Dielectric Filter in Planar Configuration," *IEEE Journal of Microwaves*, pp. 1–11, 2022.